

Christoph Busch*, Benjamin Schullcke and Knut Moeller

Realization of a multi-layer EIT-system

Abstract: Electrical Impedance Tomography (EIT) is an imaging technique used for monitoring of ventilation distribution in the lung. Small alternating currents are injected and resulting voltages are measured on the body surface with electrodes fixed around the thorax. Two-dimensional EIT (2D-EIT) is the most common technique in clinical applications but enables visualization of only one horizontal slice of the thorax. However, additional information in the cranio-caudal direction is necessary to more comprehensively assess the ventilation distribution.

3D-EIT systems address this issue, but clinically approved systems are not yet available. The aim of this study is to realize a multi-layer EIT-system with several electrode planes. An approved EIT system functions as basis for this development (PulmoVista 500, Dräger, Lübeck, Germany). Two planes were used for the technical realization of the multi-layer EIT-system. The alternation between the planes was realised using analog switches, which were controlled via a frequency generator and transfer the injected current and the measured voltages between the different electrode planes and the EIT device. The multi-layer EIT-System was applied to a phantom tank for first pilot measurements.

Results on the phantom tank with non-conductive targets at different heights reveal that the system is capable of providing information in the cranio-caudal direction. The high frame rates of EIT images combined with the high switching speed of the used analog switches enable real-time acquisition of ventilation at different thoracic planes. Thus, the modified EIT device makes it possible to comprehensively monitor the redistribution of air in the lungs during a breathing cycle, not only in a single plane, but also in the cranio-caudal direction.

Keywords: electrical impedance tomography, multi-layer EIT, medical imaging

<https://doi.org/10.1515/cdbme-2017-0060>

1 Introduction

Conventional EIT systems used in clinical routine are only able to provide two-dimensional (2D) information. However, it has been shown in several studies [1] that the assessment of ventilation distribution in cranio-caudal direction, is necessary to get a detailed insight into the lungs physiology. To enable further developments, a multi-layer EIT system based on the PulmoVista 500 (Dräger, Lübeck, Germany) shall be realized and proved.

In this paper, the setup for a multi-layer EIT, consisting of the measurements, data processing, reconstruction and evaluation, is described and realized with two layers.

2 Methods and materials

All data in this paper was recorded with the EIT-system PulmoVista 500 (Dräger, Lübeck, Germany). A phantom tank was employed as target domain for the measurements. Data processing and visualization have been carried out utilizing MATLAB R2016b (MathWorks Inc., Natick, MA, USA) and the toolbox EIDORS [2].

2.1 Measurement setup

2.1.1 Measurement setup for two-layer EIT

In a conventional 2D-EIT setup, a belt with 16-32 electrodes (n_{OE}) is used for the measurements. Thereby the electrodes are attached equidistantly in a fixed height around the thorax of the patient. To realize multi-layer EIT measurements the original measuring plane needs to be extended. For the plane expansion, a separate circuit board was used. The number of electrodes per layer is consistent and equal to the original layer. Between the layers, no variation of electrode arrangement was used, thus, electrode 1 of the first layer is below the first electrode of all other k layers. The different electrode layers, with each 16 equidistantly attached

*Corresponding author: Christoph Busch: Furtwangen University, Institute of Technical Medicine, Germany, e-mail: christoph.busch@hs-furtwangen.de

Benjamin Schullcke, Knut Moeller: Furtwangen University, Institute of Technical Medicine, Germany, e-mail: {sben, moe}@hs-furtwangen.de

electrodes, were fixed on different heights on the measurement object, as shown in **Figure 1**. Current injection and voltage measurements from the EIT-system were alternated between the different electrode planes using analog switches, whereas the original electrodes of the system were used as gateway (see **Figure 1**).

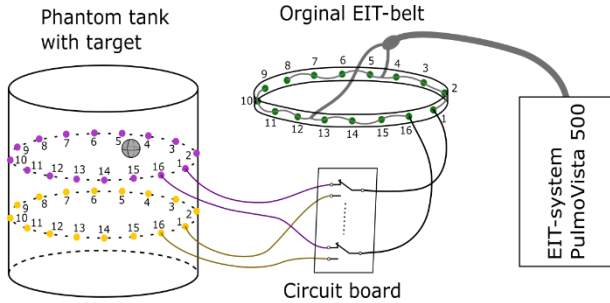


Figure 1: General measurement setup with the prototype circuit board for two-layer EIT measurements. For simplicity, only two of the 16 leads from original electrode belt to the circuit board and only four of the 32 leads from circuit board to the tank are illustrated.

The measurements were realized with a prototype circuit board which was designed to support two measurement layers (2×16 electrodes (n_E)). A phantom tank with an inner radius of 14.5 cm and an inner height of 37.5 cm was used as measuring domain. The tank was filled with 17 litres of salt water with a conductivity of 0.5 S/m. The two electrode planes were at a height of 6.6 cm and 13.3 cm. The electrodes were fixed equidistantly around the boundary.

All 32 electrodes were connected to the prototype circuit board. Analog switches of the type ADG734BRUZ (Analog Device, Norwood, MA, USA) were used for the alternation between the electrode layers. The components were supplied with ± 2.5 VDC. Further imported characteristics were a low transition resistance (2.5Ω) and a switching speed in nanosecond range.

In the measurement setup, the switching signal was realized with the help of a frequency generator (HM 8030-4, HAMEG Instruments GmbH, Mainhausen, HE, Germany). The rectangular switching signal was set to different frequencies between 1 and 15 Hz.

Copper plates were used to access the measuring signal and current injection from the original electrode belt. Therefore, each electrode contact was connected to a plate. Leads at the plates allow connection to the circuit board and the analog switches.

A non-conductive spherical target (diameter = 45.7 mm) was placed in the phantom tank. The sphere was connected to a wooden rod to ensure a fixed position. With the help of a screw clamp, the target was fastened at the tank via the rod. The position of the sphere was defined with an inner height

of 13.3 cm and 5.5 cm distance from electrode 4 to the centre of the tank.

2.1.2 Measurements without circuit board

To analyze the influence of the prototype circuit board on the EIT measurements, a reference measurement has been realized without the circuit board (1×16 electrodes). The connection of the EIT belt with the phantom tank was also achieved with copper plates as mentioned in section 2.1.1. The electrode plane was fixed on a height of 13.3 cm. The position of the target was the same as described in section 2.1.1. Therefore, only information out of one layer can be obtained.

2.2 Data processing

The measured voltages utilizing the analog switches contains the data of both electrode layers and were stored in the matrix $\mathbf{Z}^{m \times n}$. The exact matrix size of \mathbf{Z} depends on the measuring period t_m and the frame rate p_{fps} of the EIT-system ($n = t_m \cdot p_{fps}$). One column \mathbf{z}_i of \mathbf{Z} consists out of $m = n_E \cdot (n_E - 3) = 208$ voltage measurements (one frame), thus, $\mathbf{Z} = [z_{i,j}]$, with $i = 1, 2, \dots, m$ and $j = 1, 2, \dots, n$.

Since the switching of the analog switches and the measurement process of the EIT-system cannot be synchronized, the exact time point of switching is unknown. Before the multi-layer data can be visualized, the measured data needs to be separated in the particular layers.

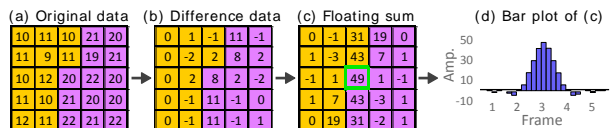


Figure 2: Example of the separation algorithm with fictional data (Yellow: first level; Purple: second level). (a) Original data (b) Finite difference approximation of (a). (c) Floating sum of one frame length of (b). (d) Bar plot of the values of (c). The maximum value defines the point of level change (green framed).

For the separation, the time point of layer changing is required. Therefore, the difference of each element of a vector \mathbf{z}_{j+1} to the correspondent element in the previous vector \mathbf{z}_j was calculated. The calculated differences were stored in matrix \mathbf{D} with the size $m \times n$. The first column of \mathbf{D} was filled with zeros (no prior values). Subsequently the floating sum of one frame length was calculated as in eq 1. The results were stored in a matrix \mathbf{P} of the size $m \times n$. The maximum value in a certain matrix section of \mathbf{P} represents the point of layer change. The section of search depends on the used switching speed in the recorded data.

$$P_{ij} = \begin{cases} \sum_{i=1}^m D_{ij}, & i = 1 \\ \sum_{i=1}^m D_{ij} + \sum_{k=1}^{i-1} D_{k,j+1}, & i > 1 \end{cases} \quad (1)$$

This separation process is only possible if the potentials of the layers differ from each other. The potential difference depends therefore on the transition resistances of the electrodes (schematic procedure of finding the point of level change in **Figure 2**). After the detection of the switching time point, it was possible to assign the measurements to different layers. To get consistent data set of each layer, the data gaps were filled with linear interpolated data.

2.3 Image reconstruction

To reconstruct the conductivity changes from measured boundary voltages, the one-step Gauss-Newton solver with the Tikhonov regularization was used.

$$\hat{\mathbf{x}} = \mathbf{B}(\lambda)\mathbf{z} \quad (2)$$

In eq 2, $\hat{\mathbf{x}}$ is the reconstructed conductivity change and vector $\mathbf{z} = \mathbf{v} - \mathbf{v}_{\text{ref}}$ the voltage difference between the measured voltage \mathbf{v} and a reference voltage \mathbf{v}_{ref} . To get a normalized time difference EIT, each element of the voltage difference \mathbf{z} was calculated as $z_i = (v_i - v_{\text{ref},i})/v_{\text{ref},i}$. The reconstruction matrix $\mathbf{B}(\lambda)$ maps the voltage difference \mathbf{z} to the change in conductivity distribution $\hat{\mathbf{x}}$. The calculation of the reconstruction matrix $\mathbf{B}(\lambda)$ depends on the hyperparameter λ which is used to control the impact of regularization (detailed in [3]). The used hyperparameter λ was set to 2.2467e-05.

2.4 Evaluation

Three techniques to evaluate the reconstructed images were considered in this study. The reconstructed EIT images $\hat{\mathbf{x}}$ were represented in 200×200 pixels. For the evaluation of the images, the 40% - amplitude set was calculated as in eq 3 for each element of $\hat{\mathbf{x}}$. The calculation leads to a binary image to focus only on the image pixels which are lower than 40% of the maximum amplitude. $\hat{\mathbf{x}}_{\text{AP}}$ thereby represents the calculated binary image [5].

$$\hat{\mathbf{x}}_{\text{AP}i} = \begin{cases} \mathbf{1}, & \text{if } \hat{\mathbf{x}}_i \leq 0.4 \cdot \max(\hat{\mathbf{x}}) \\ \mathbf{0}, & \text{otherwise} \end{cases} \quad (3)$$

The following performance measurements were calculated with respect to $\hat{\mathbf{x}}_{\text{AP}}$:

Position error (PE): Measures the PE of the centre of gravity (CoG) of the reconstructed image in relation to the

image target with respect to the tank centre with $\text{PE} = r_{\text{GT}} - r_{\text{AP}}$. Thereby r_{GT} and r_{AP} represent the distance of CoG to the centre of the tank (r_{GT} - ground truth; r_{AP} - 40% - amplitude set). PE is expected to be close to zero.

Shape deformation (SD): This method compares the reconstructed shape of $\hat{\mathbf{x}}_{\text{AP}}$ with the shape of ground truth (GT). Therefore, the difference of the images was calculated. That the PE will not influence the evaluation of the SD, the area of GT was placed on the CoG of $\hat{\mathbf{x}}_{\text{AP}}$ (shifting of GT). The SD gives a ratio of the difference image to the reconstructed 40% - amplitude set through, $\text{SD} = \sum_{i \in C} [\hat{\mathbf{x}}_{\text{AP}}]_i / \sum_i [\hat{\mathbf{x}}_{\text{AP}}]_i$, where C represents the shifted GT. SD is expected to be small.

Relative reconstruction error (RE): RE gives a ratio for the ℓ_2 -norm of the difference image to the ℓ_2 -norm of the ground truth $\hat{\mathbf{x}}_{\text{GT}}$, thus, $\text{RE} = \|\hat{\mathbf{x}} - \hat{\mathbf{x}}_{\text{GT}}\|_2 / \|\hat{\mathbf{x}}_{\text{GT}}\|_2$. RE is expected to be small [6].

3 Results

Figure 3 (a) shows the ground truth conductivity change. The reconstructed conductivity changes are depicted in **Figure 3 (b)** and **Figure 3 (c)** with and without the circuit board, respectively. **Figure 3** (lower row) visualizes measurement layer one and **Figure 3** (upper row) measurement layer two. The measurements with the circuit board were recorded with a switching frequency of 5 Hz. It is apparent, that both measurement reconstructions show nearly the same images in the second layer.

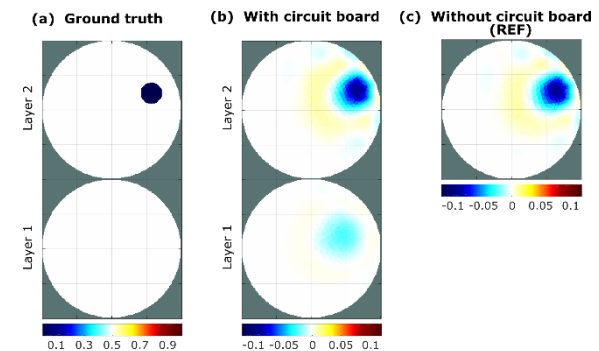


Figure 3: Reconstructed images of both measurement layers. (a) Ground truth. (b) Reconstructed measurements with the used circuit board. (c) Reconstructed measurements without the used circuit board (reference measurement).

The measurement setup with the circuit board and the used EIT device allows only a certain switching frequency. The faster the switching, the more incomplete frames were received by interrupting the measurements through a layer change. The graph in **Figure 4** shows the relation between

the intact frames per second (fps) and the used switch frequency. This relation was plotted with three different EIT frame rates (30, 40 and 50 fps). It is observed, that with all configured frame rates the number of intact fps is decreasing over increasing the switching speed. With the set frame rate of 50 fps, the number of intact fps is the highest.

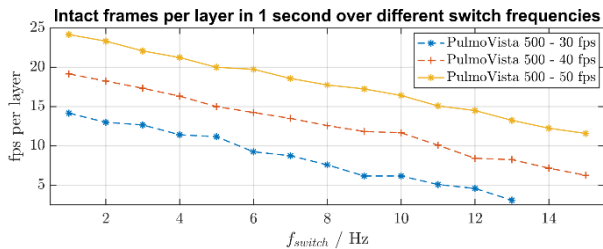


Figure 4: The relation of intact frames per second (fps) of each layer over different switch frequencies with the three adjusted frame rates 30, 40 and 50 fps at the EIT-system. Shown are the mean values of each six samples. The blue dashed line with stars represents an EIT image frame rate of 30 fps. The red dashed line with crosses stands for an EIT image frame rate of 40 fps. The yellow line with stars represents the EIT image frame rate 50 fps.

The evaluation parameters of the reconstructions are shown in **Table 1**. The comparison of the values of both measurements shows small variations. Through the calculated 40% - amplitude set, the sphere is not visible in the bottom layer with the circuit board. Therefore, no performance parameters of this layer can be shown.

Table 1: Performance measurements (PM): PE and SD of the reconstructed 40% - amplitude images, RE of the reconstruction image to ground truth

PM	Rec. with circuit board		Rec. without circuit board	
	Layer 1	Layer 2	-	Layer 2
PE	-	-1.29 cm	-	-1.16 cm
SD	-	0.2914	-	0.3081
RE	0.0409	0.0878	-	0.0854

4 Discussion

In this study, an approach of a multi-layer EIT-system was considered and developed to get more information in cranio-caudal direction. As **Figure 3 (b)** and **Figure 3 (c)** illustrates, both measurements lead to nearly similar reconstructions in the second layer. Nevertheless, it can be illustrated in **Figure 3** that the prototype circuit board has no detrimental effects on the reconstructed images and provides an additional measurement layer.

The PE of the reconstruction without the circuit board is closer to zero than under the usage with the circuit board. For the two different measurements, the position of the inner target had to be positioned newly by hand for each measurement setup. Therefore, there is always a position error between the different measurements and it is not possible to assign the difference of the PE to the circuit board. The values of the SD and of the RE are in both reconstructions relatively small. Summarized, the performance parameters clarify a negligible difference between the measurement setups.

The highest switching frequency which facilitates the most intact fps was reached with 13 Hz at 50 fps of EIT images. Therefore, only 13 Hz are feasible, if the separation algorithm needs at least one complete frame.

5 Conclusion

The additional information in cranio-caudal direction through a second layer can lead to more precise statements about the inner conductivity distribution. Based on the results we expect that the development of a four-layer system can be realized similarly.

Author's Statement

Research funding: This work was partially supported by the Federal Ministry of Education and Research (BMBF) under grand no. 03FH038I3 (MOSES). Conflict of interest: Authors state no conflict of interest. Informed consent: Informed consent is not applicable. Ethical approval: The conducted research is not related to either human or animals use.

References

- [1] Krueger-Ziolek S, Schullcke B, Zhao Z, et al. Multi-layer ventilation inhomogeneity in cystic fibrosis. *Resp Phys.* 2016; 233:25-32.
- [2] Adler A, Lionheart WR. Uses and abuses of EIDORS: an extensible software base for EIT. *Physiol Meas.* 2006; 27:S25-S42.
- [3] Adler A, Guardo R. Electrical impedance tomography: regularized imaging and contrast detection. *IEEE trans medi imag.* 1996; 15:170-179.
- [4] Adler A, Arnold JH, Bayford R, et al. GREIT: a unified approach to 2D linear EIT reconstruction of lung images. *Physiol Meas.* 2009; 30:S35-S55.
- [5] Gong B, Schullcke B, Krueger-Ziolek S, et al. Sparse regularization for EIT reconstruction incorporating structural information derived from medical imaging. *Physiol Meas.* 2016; 37:843-862.